Delft University of Technology

Effect of amplitude and number of repetitions of the perturbation on system identification of human balance control during stance

Schut, I. M.; Pasma, J. H.; De Veij Mestdagh, J.C.; Kooij, H. Van Der; Schouten, A. C.

Important note
To cite this publication, please use the final published version (if applicable).
Please check the document version above.

Effect of Amplitude and Number of Repetitions of the Perturbation on System Identification of Human Balance Control During Stance

I. M. Schut, J. H. Pasma, J. C. De Veij Mestdagh, H. Van Der Kooij, and A. C. Schouten

Abstract—To unravel the underlying mechanisms of human balance control, system identification techniques are applied in combination with dedicated perturbations, like support surface translations. However, it remains unclear what the optimal amplitude and number of repetitions of the perturbation signal are. In this study we investigated the effect of the amplitude and number of repetitions on the identification of the neuromuscular controller (NMC). Healthy participants were asked to stand on a treadmill while small continuous support surface translations were applied in the form of a periodic multisine signal. The perturbation amplitude varied over seven conditions between 0.02 and 0.20 m peak-to-peak (ptp), where 6.5 repetitions of the multisine signal were applied for each amplitude, resulting in a trial length of 130 sec. For one of the conditions, 24 repetitions were recorded. The recorded external perturbation torque, body sway and ankle torque were used to calculate both the relative variability of the frequency response function (FRF) of the NMC, i.e., a measure for precision, depending on the noise-to-signal ratio (NSR) and the nonlinear distortions. Results showed that the perturbation amplitude should be minimally 0.05 m ptp, but higher perturbation amplitudes are preferred since they resulted in a higher precision, due to a lower noise-to-signal ratio (NSR). There is, however, no need to further increase the perturbation amplitude than 0.14 m ptp. Increasing the number of repetitions improves the precision, but the number of repetitions minimally required, depends on the perturbation amplitude and the preferred precision. Nonlinear contributions are low and, for the ankle torque, constant over perturbation amplitude.

Index Terms—Human balance control, nonlinear distortions, precision, relative variability, system identification.

I. INTRODUCTION

HUMAN balance control is essential to keep the human body upright in the gravitational field. Deviations from the upright position can be caused by internal and external disturbances, such as breathing and pushes against the body respectively. The central nervous system (CNS) receives sensory information about deviations from the upright position and generates stabilizing corrective ankle torques by sending motor commands to the muscles. Balance control is often described using a simplified model consisting of a single inverted pendulum representing the human body (B), pivoting around the ankle axes, controlled by a neuromuscular controller (NMC) representing the CNS and the muscles, forming a closed loop control system [1]–[3].

To quantify the contribution of the NMC to balance control, system identification techniques are used, thereby typically applying continuous anterior-posterior translations of the support surface to perturb the human body, while measuring the response in terms of body sway and ankle torque [1], [2], [4]–[10]. Alternatively, pushes against the body at the hip and/or shoulders are used as perturbations while measuring the EMG response and body sway [11]–[14]. The perturbation signal is repeated several times in one or more trials. However, no consistency exists on the perturbation amplitude and the number of repetitions required. The used peak-to-peak (ptp) perturbation amplitude ranges from 0.05 to 0.23 m for support surface translations, from 1 to 16 Nm for torques at the ankle joint or from 0.04 to 0.15 m for displacements of the hip or shoulder pushes. The used number of repetitions varies from 4 to 54. The length of one perturbation signal depends on the lowest excited frequency, resulting in recording lengths of 10 to 720 s in total. However, there are no studies investigating the effect of the perturbation amplitude and the number of repetitions on the quality of the estimated NMC. On one hand, the perturbation amplitude must be high enough to reach a low noise-to-signal ratio (NSR), and the number of repetitions must be high enough to allow for averaging, thereby both improving the quality of the estimated NMC. On the other hand, the perturbation amplitude must be low enough so participants can withstand the perturbation without stepping, and the number of repetitions must be low enough to avoid artefacts due to fatigue.

Another important aspect to consider is the nonlinear behavior of human balance control. Since human balance control is often considered as linear feedback control [1], [15]–[19], linear system identification techniques can be used. However, nonlinear responses affect the linear estimation of the NMC since parts of the signal are transferred to other frequencies [20]. Nonlinearities can be either odd, which generate power on odd harmonics of the excited frequency, or even, which generate power on the even harmonics of the excited frequencies. By using linear system identification techniques in combination with random perturbation signals however, nonlinearities are often not accurately characterized because they cannot be separated from the noise. Therefore, it is important to know how the nonlinear distortions change with perturbation amplitude. Using periodic perturbation signals, van der Kooij et al. [1] showed that the linear response of both body sway and ankle torque increased with increasing perturbation amplitude. However, only two moderate perturbation amplitudes were used.

In this study, we separated the nonlinear contributions from the noise using linear system identification techniques with specific periodic perturbation signals according to the methods of Pintelon and Schoukens [21] on healthy participants; a method that is not often used in the field of human balance control. This method allows us to 1) estimate the NMC, 2) quantify the relative variability of the estimation, i.e. a measure for precision, as a function of perturbation amplitude and number of repetitions, and 3) quantify both odd and even nonlinear contributions as a function of perturbation amplitude. The results of this study will help researchers to select an appropriate perturbation amplitude and number of repetitions to estimate the NMC, allowing for the investigation of the underlying changes in balance control due to ageing or pathologies, such as Parkinson's disease and stroke.

II. METHODS

A. Participants

Twelve healthy volunteers (six women, median age 26 years, range 24-65 years, height 1.73 ± 0.09 m, weight 73.67 ± 14.19 kg) participated in the study. The study was approved by the Human Research Ethics Committee of the Delft University of Technology (The Netherlands) and was in accordance with the Declaration of Helsinki (59th WMA General Assembly, Seoul, Republic of Korea, October 2008). All participants gave written informed consent.

B. Apparatus and Recording

Standing balance was perturbed in anterior-posterior direction with support surface translations applied by an instrumented split belt treadmill (GRAIL, Motekforce Link, Amsterdam, The Netherlands), where both belts moved in synchrony. Participants wore comfortable flat shoes and a safety harness to prevent fall injuries, without constraining normal body sway or providing support or body-oriented information. Two 6-DOF force plates embedded in the treadmill recorded ground reaction forces of each foot at a sample frequency of 1000 Hz. Eight retroreflective markers were attached to the participants' acromioclavicular joints, major trochanters, lateral epicondyles and lateral malleoli of both left and right side. Additional markers were placed on each treadmill belt. Ten motion capture cameras (Vicon Bonita, Vicon Motion Systems, Oxford, United Kingdom) surrounding the treadmill recorded the marker positions at a sample frequency of 100 Hz. Approximately 2 m in front of the treadmill a grid of 0.2 by 0.2 m was projected on a semi-cylindrical screen, at which participants could focus their gaze.

C. Perturbation Signal

The perturbation was a random-phase multisine signal with a period of 20 s, designed to excite 18 specific odd frequencies between 0.05 and 5 Hz at an interleaved logarithmic frequency grid, since changes in human balance control are most pronounced in the frequency range of 0-3 Hz [5]. The multisine has a flat velocity spectrum, except for the magnitude of the first excited frequency (0.05 Hz), which was 1/3 of the magnitude of the second excited frequency (0.15 Hz), to prevent dominance of the lowest frequency in the belt movement. The unexcited odd and even harmonics enable analysis of the nonlinear contributions [20], [22]–[24]. The amplitude and the number of repetitions of the 20 s multisine varied between conditions, see procedures.

D. Procedures

Participants were instructed to stand as normal as possible without moving their feet, with eyes open and the arms crossed in front of the chest. Prior to the perturbation trials, a static trial of 5 s was recorded to calculate the length of the pendulum, i.e. the height of the center of mass (CoM) above the ankle joint. Subsequently, participants performed three practice trials of 60 s, with a low, middle (mid) and high perturbation amplitude of 0.02, 0.08 and 0.2 m ptp respectively.

To study the effect of the amplitude of the perturbation signal to the relative variability of the NMC estimation, the perturbation amplitude varied over seven conditions, ranging from 0.02 m ptp (A2) to 0.2 m ptp (A20) (table I). For each condition, 6.5 periods of the multisine were recorded, resulting in a trial length of 130 s. All conditions were recorded once, except for the A8 condition which was recorded 4 times to study the effect of the number of repetitions on the relative variability of the NMC estimation. All 10 trials were presented in random order. Between each trial, participants could take an optional break of 1 minute.

E. Data Processing

Data were processed in Matlab version R2016b (MathWorks, Natick, MA, USA). Force plate data were resampled to 100 Hz to match the sample frequency of the marker data.

The marker and force plate data from the static trial were used to calculate the length of the pendulum according to Winter et al. [25], and the mass of the participant respectively.

The first 10 s of the data from the perturbation trials were discarded to remove transient effects, leaving 120 s of data. The data were cut in 6 segments of 20 s, i.e. the length of

Con.	Pos. ptp (m)	Acc. max (m/s²)	D_{ext} max (Nm)	BS ptp (°)	Nr. Tr.	Nr. Rep. Rec.	Nr. Rep. An.
A2	0.02	0.87	48.67	1.09	1	6.5	6
A5	0.05	1.39	80.88	2.17	1	6.5	6
A8	0.08	2.25	151.84	3.12	4	26	24
A11	0.11	3.22	205.20	3.92	1	6.5	6
A14	0.14	3.88	257.23	4.80	1	6.5	6
A17	0.17	4.41	291.35	5.59	1	6.5	6
A20	0.20	4.79	340.01	6.56	1	6.5	6

Seven conditions (Con.) of the perturbed trials with corresponding peak-to-peak (ptp) position (Pos.), participants mean maximal acceleration (Acc.), participants mean maximal perturbation torque (D_{ext}), participants mean ptp body sway (BS), number of trials (Nr. Tr.), number of recorded repetitions of the perturbation signal (Nr. Rep. Rec.) and number of repetitions available for analysis (Nr. Rep. An.).

one period of the multisine. Position of the CoM was derived from the marker positions. Body sway (BS), i.e. the angle of the CoM with respect to the vertical, was calculated using the CoM position in anterior-posterior direction and the length of the pendulum. The Centre of Pressure with respect to the ankle position (CoP) of both feet was used to calculate the left and right ankle torque with inverse dynamics [26]. Total ankle torque was calculated by the sum of both left and right ankle torque.

Translations of the belt position resulted in an external torque perturbing human standing balance according to [5]

$$D_{ext}(t) = -m_{com}l_{com}\ddot{x}_{ss}(t) \tag{1}$$

in which $\ddot{x}_{ss}(t)$ is the acceleration of the support surface derived from the belt markers, l_{com} is the length of the pendulum and m_{com} is the mass of the pendulum, i.e. the mass of the participant minus the mass of the feet [25].

F. Data Analysis

For the data analysis, the Matlab toolbox provided by Pintelon and Schoukens [21] was used. The perturbation torque $D_{ext}(t)$, body sway $BS(t)$ and ankle torque $T(t)$ were transformed to the frequency domain using the fast Fourier transform (FFT) and divided into periodic responses and nonperiodic noise. The periodic response $D_{ext}(f)$, $BS(f)$ and $T(f)$ respectively, were obtained by averaging the FFT over all segments. The nonperiodic noise $D_{ext,n}(f)$, $BS_n(f)$ and $T_n(f)$ are different for each segment and are defined as the remnants after subtracting the mean FFT from each segment. The power spectral densities (PSDs) were calculated for both the periodic responses and the nonperiodic noise. The dynamics of the NMC are described by the frequency response function (FRF), i.e. the relation between body sway and ankle torque, in terms of a magnitude and phase [2], [5], [6], [27]. The FRF can be defined as

$$G(f) = G_0(f) + G_B(f) + G_S(f) + N_G(f) \tag{2}$$

in which $G_0(f)$ is the underlying linear system, $G_B(f)$ is the bias due to the nonlinear distortions, $G_S(f)$ are the stochastic nonlinear contributions and $N_G(f)$ are the errors due to the output noise [20].

1) Best Linear Approximation: The underlying linear system combined with the bias due to nonlinear distortions defines the best linear approximation (BLA)

$$G_{BLA}(f) = G_0(f) + G_B(f) \tag{3}$$

Since the perturbation signal is periodic, the $G_{BLA}(f)$ of the NMC can be estimated by

$$G_{BLA}(f_{ex}) = -\frac{T(f_{ex})}{BS(f_{ex})} \tag{4}$$

in which f_{ex} are the excited frequencies [1], [28].

2) Relative Variability of the Best Linear Approximation: The sample variance of the estimated BLA is defined as [22]

$$\sigma_G^2(f_{ex})$$
$$= \frac{|G_{BLA}(f_{ex})|^2}{P}$$
$$\times \left(\frac{\sigma_{T_n}^2(f_{ex})}{|T(f_{ex})|^2} + \frac{\sigma_{BS_n}^2(f_{ex})}{|BS(f_{ex})|^2} - 2Re\frac{\sigma_{T_nBS_n}^2(f_{ex})}{T(f_{ex})BS(f_{ex})} \right) \tag{5}$$

where P is the number of repetitions, $\sigma_{X_n}^2(f_{ex})$ is the variance of the nonperiodic noise of the body sway or ankle torque and $\sigma_{T_nBS_n}^2(f_{ex})$ is the covariance of the body sway and ankle torque according to

$$\sigma_{X_n}^2(f_{ex}) = \frac{1}{P-1}\sum_{p=1}^{P}\left|X_n^p(f_{ex})\right|^2 \tag{6}$$

$$\sigma_{T_nBS_n}^2(f_{ex}) = \frac{1}{P-1}\sum_{p=1}^{P}T_n^p(f_{ex})\cdot conj(BS_n^p(f_{ex})) \tag{7}$$

where p denotes the repetition index. The first and second term within the brackets of (5) represent the NSR of the nonperiodic noise of the ankle torque (NSR_T) and body sway (NSR_{BS}) respectively. The third term represents the correlation between both signals (NSR_{TBS}).

Equation (5) was rewritten to define the relative variability ε, which is described by the ratio between the sample standard deviation ($\sigma_G(f_{ex})$) and $G_{BLA}(f_{ex})$

$$\varepsilon = \sqrt{\frac{\overline{\sigma_G^2}}{|G_{BLA}|^2}} = \sqrt{\frac{1}{P}\overline{\sum NSR}} \tag{8}$$

with $\sum NSR$ the sum of the three terms between brackets in (5), i.e. NSR_T, NSR_{BS} and NSR_{TBS}. The bars indicate averaging over the excited frequencies and participants. ε indicates how much nonperiodic noise is left after averaging the segments, relative to $G_{BLA}(f_{ex})$. An ε of 0 indicates a perfect estimator without noise, i.e. no relative variability and thus high precision. An ε of 1 indicates a poor estimator with a high relative variability where the noise level is of the same order as the magnitude of $G_{BLA}(f_{ex})$, i.e. low precision. According to (8), the relative variability of the estimated $G_{BLA}(f_{ex})$ can be influenced by both the number of repetitions and the NSR, which itself can be influenced by the perturbation amplitude.

Equation (8) was used to calculate the required number of repetitions P_ε to reach given ε of 0.02, 0.05, 0.10 and 0.15

$$P_\varepsilon = \frac{\sqrt{\sum NSR}}{\varepsilon^2} \quad (9)$$

P_ε was calculated for each perturbation amplitude on a low frequency range of 0.05-0.95 Hz, mid frequency range of 1.00-2.35 Hz and high frequency range of 2.40-4.95 Hz.

To check the calculated number of repetitions required to reach ε of 0.02, 0.05, 0.10 and 0.15, a technique called bootstrapping was used [28]. For each number of repetitions, ε was calculated according to (8) using x randomly chosen repetitions, with x ranging from 1-23, out of the recorded data of 24 repetitions at the A8 conditions. This process was repeated 100 times, over which the mean and standard deviation were calculated.

3) Quantifying Nonlinear Distortions: Since it is not possible to quantify the bias due to nonlinear distortions ($G_B(f)$), which affects the estimation of $G_{BLA}(f)$, the stochastic nonlinear contributions ($G_S(f)$), which are of the same order as $G_B(f)$, were calculated according to Pintelon and Schoukens [21].

First, the relative stochastic nonlinear contributions on the perturbation torque, body sway and ankle torque were calculated, by looking at the odd and even unexcited harmonics. When the power on the unexcited harmonics was twice as large as the variance on those frequencies, the stochastic nonlinear contributions were detectable [22]. Stochastic nonlinear contributions in the perturbation torque indicate nonlinearities due to the treadmill. The periodic responses of the body sway and ankle torque were corrected at the unexcited harmonics for those impurities in the perturbation torque by

$$BS_c(f_u) = BS(f_u) - D_{ext}(f_u) \cdot \frac{B(f_u)}{1 + B(f_u)NMC(f_u)} \quad (10)$$

$$T_c(f_u) = T(f_u) - D_{ext}(f_u) \frac{B(f_u)NMC(f_u)}{1 + B(f_u)NMC(f_u)} \quad (11)$$

where f_u represents the unexcited frequencies and $B(f_u)$ represents the rigid human body dynamics [21]. Any remaining power on the unexcited frequencies is caused by the human. The relative stochastic nonlinear contributions of the body sway and ankle torque were calculated as a percentage by respectively averaging the power of the corrected body sway and corrected ankle torque over low, mid and high frequencies, dividing to the total power, and multiplying by 100.

Second, the relative stochastic nonlinear contributions on the body sway and ankle torque were used to calculate $G_S(f_{ex})$, which was compared to $N_G(f_{ex})$, both calculated according to Pintelon and Schoukens [21].

4) Variance Accounted For: To study the effect of both the relative variability and nonlinear distortions ($G_B(f_{ex})$), we calculate how well the estimated linear model $G_{BLA}(f_{ex})$ describes the measured data, using the variance accounted for (VAF). The modeled ankle torque was calculated according

$$T_{mod}(f_{ex}) = \frac{1}{P} \sum_{p=1}^{P} (BS(f_{ex}) \cdot G_{BLA}(f_{ex})) \quad (12)$$
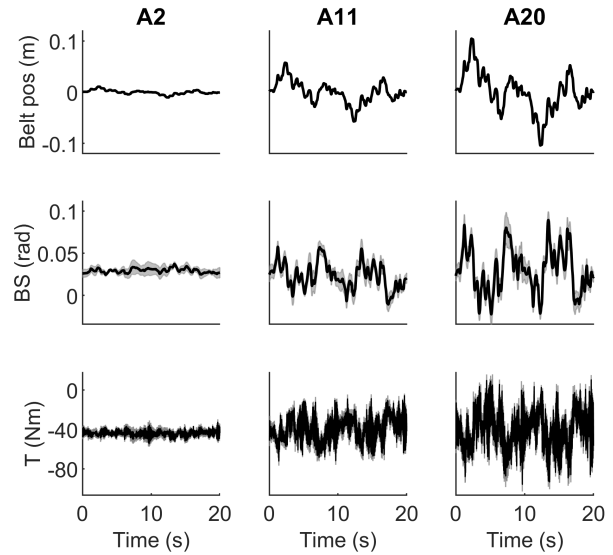
Fig. 1. Time series of a typical participant. Mean (black) and standard deviation (grey) over 6 segments of the belt position (upper row), body sway (BS) (middel row) and ankle torque (T) (bottom row) are shown for the A2, A11 and A20 condition.

and converted to the time domain using the inverse Fourier transform

$$T_{mod}(t) = \mathcal{F}^{-1}(T_{mod}(f_{ex})) \quad (13)$$

The VAF was calculated according

$$VAF = \left(1 - \frac{var(\overline{T(t)} - \overline{T_{mod}(t)})}{var(\overline{T(t)})}\right) \cdot 100\% \quad (14)$$

where $\overline{T(t)}$ and $\overline{T_{mod}(t)}$ are the recorded ankle torque and modeled ankle torque respectively, both averaged over 6 segments and filtered with a second order butterworth lowpass filter with a cutoff frequency of 5 Hz. A VAF of e.g. 100% indicates that 100% of the measured data can be explained by the linear system $G_{BLA}(f_{ex})$. The VAF values can be decreased by the bias due to nonlinear distortions ($G_B(f_{ex})$) or remaining noise after averaging over 6 segments.

III. Results

The time series and corresponding PSD of the perturbation torque, corrected body sway and corrected ankle torque of a typical participant are shown in Fig 1 and Fig 2.

A. Relative Variability of the Best Linear Approximation

Fig 3 shows the estimated FRF of $G_{BLA}(f)$ and σ_G averaged over the participants, both normalized for the gravitational stiffness, i.e. mass of the pendulum multiplied by the length of the pendulum and the gravitational constant ($m_{com}l_{com}g$), to eliminate the effect of participants mass and height. The ratio between σ_G and $G_{BLA}(f)$, i.e. ε, decreases by increasing the perturbation amplitude (Fig 3) due to lower NSR of the nonperiodic noise on those perturbation amplitudes (Fig 4). However, at higher perturbation amplitudes, ΣNSR seems to flatten out.
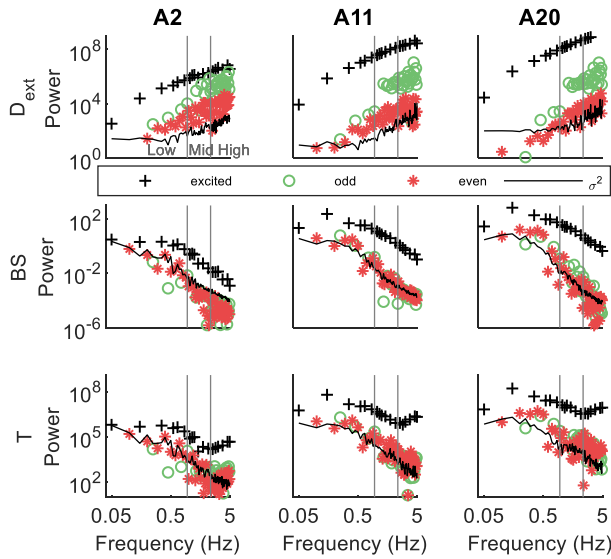
Fig. 2. Power spectral densities (PSDs) of the perturbation torque (upper row), body sway (middle row), corrected for impurities in the perturbation torque, and ankle torque (bottom row), corrected for impurities in the perturbation torque, for the A2, A11 and A20 condition of one typical participant, presented by the mean power over the 6 segments of the excited (+, black), unexcited odd (o, green) and unexcited even (∗, red) frequencies. The solid black line represents the variance over the 6 segments of the excited and unexcited frequencies. The three areas between the two vertical grey lines represent the three frequency groups.
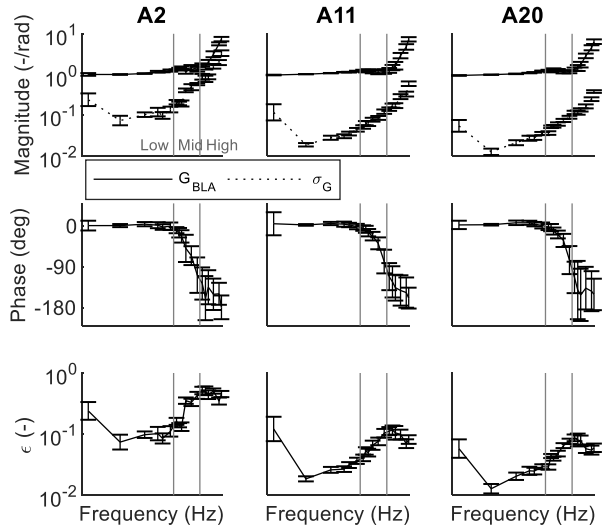
Fig. 3. Mean and standard deviation over all participants of the magnitude of G_{BLA} (upper row, solid) and square root of the sample variance (σ_G) (upper row, dotted), both normalized for the gravitation force, phase of G_{BLA} (middle row) and relative variability ε (bottom row) for the A2, A11 and A20 condition. The three areas between the two vertical grey lines represent the three frequency groups.

Table II shows, for each frequency group, the required values for P_ε, given a certain perturbation amplitude and ε of 0.02, 0.05, 0.10 and 0.15. Both higher perturbation amplitudes, i.e. due to the decreasing NSR, and higher numbers of P_ε result in a lower ε. Note however that at the higher perturbation amplitudes, a lower ε can only be obtained by increasing P_ε and not by further increasing the perturbation amplitude due to the flattened NSR.
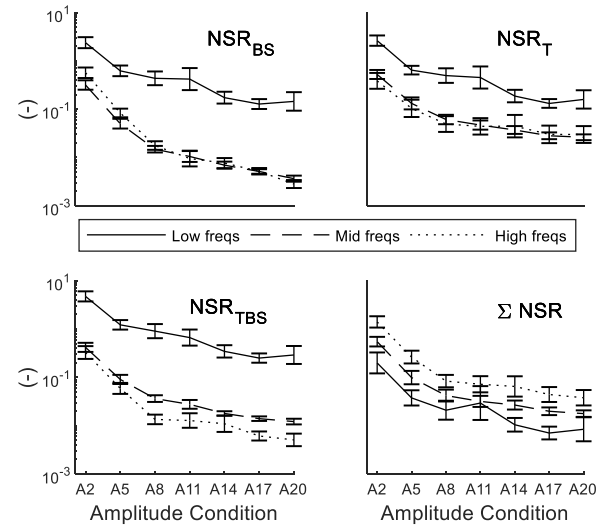
Fig. 4. Mean and standard deviation over all participants of NSR_{BS} (top left), NSR_T (top right), the correlation term (bottom left) and the summation of the three terms ($NSR_{BS}+NSR_T-NSR_{TBS}$) (bottom right) for all amplitude conditions. For each term, the results are plotted for the low (solid), mid (dashed) and high (dotted) frequency range.

TABLE II
REQUIRED NUMBER OF REPETITIONS

Frequency group	Amplitude (m ptp)	ΣNSR (-)	Nr. repetitions to obtain relative variability ε of			
			.02	.05	.10	.15
Low [0.05-0.95] Hz	A2	0.199	497	80	20	9
	A5	0.038	94	15	4	2
	A8	0.021	52	8	2	1
	A11	0.029	74	12	3	1
	A14	0.010	26	4	1	-
	A17	0.007	18	3	1	-
	A20	0.008	21	3	1	-
Mid [1.00-2.35] Hz	A2	0.548	1370	219	55	24
	A5	0.099	247	40	10	4
	A8	0.042	105	17	4	2
	A11	0.032	79	13	3	1
	A14	0.027	67	11	3	1
	A17	0.020	50	8	2	1
	A20	0.018	44	7	2	1
High [2.40-4.95] Hz	A2	1.404	3510	562	140	62
	A5	0.263	657	105	26	12
	A8	0.084	209	33	8	4
	A11	0.072	180	29	7	3
	A14	0.065	162	26	6	3
	A17	0.044	110	18	4	2
	A20	0.038	95	15	4	2

Calculated number of repetitions (P_ε) required to obtain a certain relative variability ε, given a specific perturbation amplitude and frequency range.

Fig 5 shows the calculated ε using the bootstrap method (ε_b) together with the calculated ε corresponding to table II (ε_t). Both ε are comparable although ε_b is around 0.02 lower than ε_t at the high frequency range.

B. Quantifying Nonlinear Distortions

Fig 6 shows the estimated relative stochastic nonlinear contributions on the unexcited odd and even harmonics for the corrected body sway and corrected ankle torque. The relative
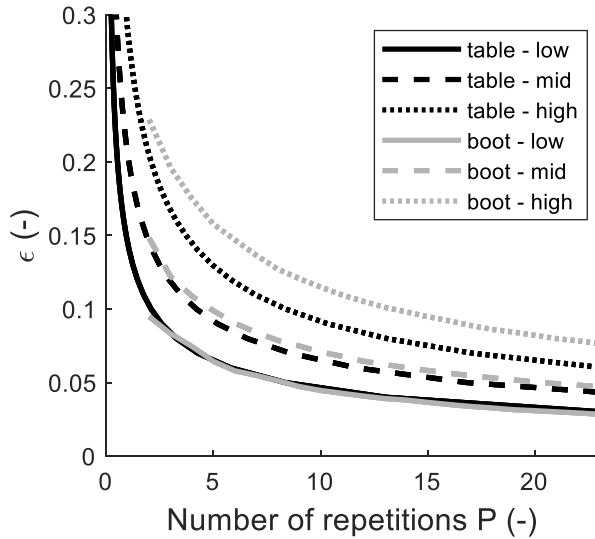
Fig. 5. Mean over 100 relative variabilities (ε) calculated with the bootstrap method (ε_b)(grey) for low (solid), mid (dashed) and high (dotted) frequencies. The calculated ε corresponding to Table II (ε_t) are shown in black for low (solid), mid (dashed) and high (dotted) frequencies.
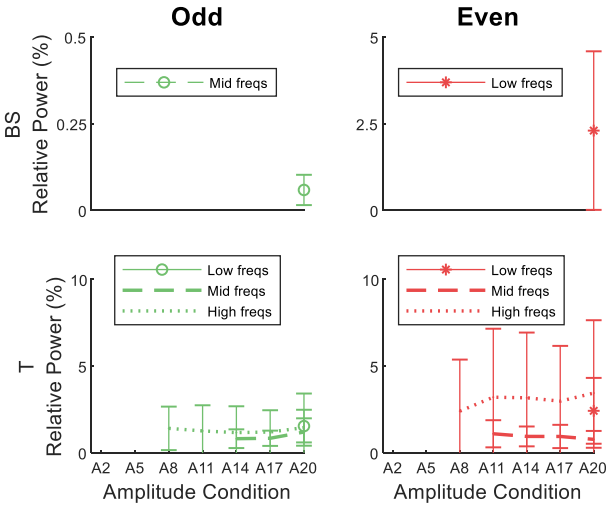
Fig. 6. Mean and standard deviation over all participants of the relative stochastic odd (left) and even (right) nonlinear contributions in the corrective body sway (top) and corrective ankle torque (bottom). The results are plotted for low (solid), mid (dashed) and high (dotted) frequencies. Note the different scales on the y-axis.

stochastic nonlinear contributions are only shown for those perturbation amplitudes where the stochastic nonlinear contributions were detectable.

For the corrected body sway the power on the odd and even unexcited harmonics is too low to detect any stochastic nonlinear contributions. Only at A20 stochastic nonlinear contributions could be detected in the lower and mid frequencies, although not contributing more than 0.1% for odd and 2.3% for even harmonics.

In the corrected ankle torque, both odd and even relative stochastic nonlinear contributions are highest on the high frequencies (1.1-1.5% and 2.4-3.4% respectively), but they are also present on the mid frequencies (0.7-1.2%). For the lower frequencies, the stochastic nonlinear contributions could only be detected for the A20 condition, where the contributions are
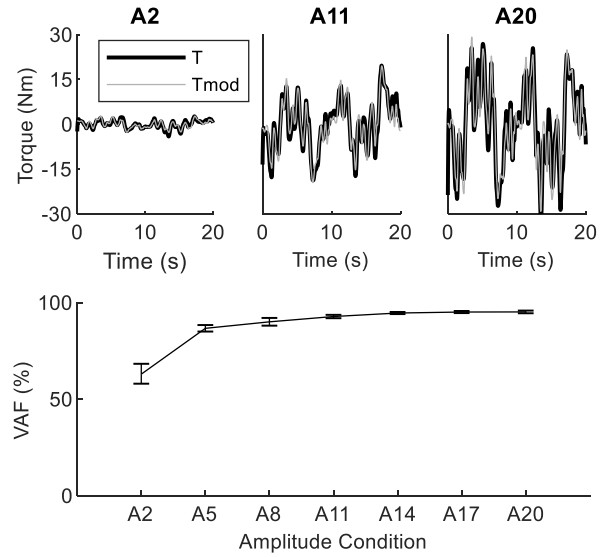
Fig. 7. (Top) Filtered measured ankle torque (black) and filtered modeled ankle torque (grey) of one typical participant for the A2, A11 and A20 condition. (Bottom) Mean and standard deviation over all participants of the Variance Accounted For (VAF) for all amplitude conditions.

1.5% (odd) and 2.4% (even). When increasing the perturbation amplitude, both odd and even relative stochastic nonlinear contributions do not change.

$G_S(f_{ex})$, i.e. the stochastic nonlinear contributions of body sway and ankle torque together, was as large as $N_G(f_{ex})$ (both not shown) for almost all perturbation amplitudes, meaning that $G_S(f_{ex})$ is of the same level as noise. Moreover, $G_S(f_{ex})$ was for none of the perturbation amplitudes twice as large as the noise $N_G(f_{ex})$ and thus not detectable.

C. Variance Accounted For

Fig 7 shows the filtered ankle torque and modeled ankle torque, averaged over the segments of the A2, A11 and A20 condition for one typical participant. The averaged VAF over all participants increases from 63±15% to 95±2% by increasing the perturbation amplitude (Fig 7, bottom row) and flattens out at A14.

IV. DISCUSSION

In this paper we used a specific periodic perturbation signal to study the effect of the perturbation amplitude and the number of repetitions on the estimation of the NMC with respect to the precision and nonlinear contributions. Since both perturbation amplitude and the number of repetitions have an effect on the precision of the estimator, the required number of repetitions to reach a certain relative variability was calculated given a specific perturbation amplitude. In addition, the relative stochastic nonlinear contributions were quantified and the variance accounted for was calculated, indicating how well the linear estimator of the NMC explained the measured data.

A. Precision of the Best Linear Approximation

Both increasing the perturbation amplitude and the number of repetitions of the perturbation signal resulted in a higher

precision, indicating an improvement of the estimation of the NMC.

Table II shows that the minimal perturbation amplitude that can be used is A5 since ΣNSR is too high for amplitudes lower than A5, thereby requiring hundreds of repetitions of the perturbation signal. Higher perturbation amplitudes result in a lower ΣNSR and are therefore preferred over lower perturbation amplitudes. However, since the ΣNSR flattens out above A14, it is better to increase the number of repetitions than to increase the perturbation amplitude in order to further improve the precision of the estimator.

Unfortunately, researchers are often limited to lower perturbation amplitudes due to physical limitations of the participants such as fatigue or the inability to withstand higher perturbation amplitudes. To still reach an acceptable precision, more repetitions of the perturbation signal are required. Table II helps the researcher selecting the required number of repetitions. Researchers have to decide what ε is acceptable in a low, mid or high frequency group, depending on the expected changes in the NMC of the participant group of interest, and in what frequency group those changes are most pronounced.

Researcher should keep in mind that for each perturbation amplitude, the ΣNSR of the nonperiodic noise is different for the low, mid and high frequencies. Therefore, when choosing a proper number of repetitions to obtain a certain precision in one frequency range, the precision might be worse in another frequency range.

The measured ε using the bootstrap method were 0.02 lower than calculated in Table II at the high frequencies. This difference could be explained by higher variance of the FRF in the high frequency range. Since the variance at these frequencies is large, it is important to keep in mind that it seems that even more repetitions than stated in Table II are required to reach a certain ε in this frequency range.

Our findings are comparable with van der Kooij et al. [1] showing more power in the PSD of the body sway and ankle torque and a decrease in NSR$_{BS}$ and NSR$_T$ when increasing the perturbation amplitude from 0.06 m ptp to 0.08 m ptp. In addition, the correlation between the nonperiodic noise of the body sway and ankle torque (not shown) was high up to 1 Hz, with similar values to van der Kooij et al. This correlation suggests that the dominant source of the noise occurred inside the feedback loop, i.e. the human. The physiological cause could be the imperfect processing of noisy sensory signals, time variant behavior due to fatigue or adaption, or to other discontinuous control mechanisms [1].

The used peak-to-peak perturbation amplitudes of other studies ranging from 0.05 to 0.23 m for the support surface translations [1], [2], [4]–[10] and perturbation amplitudes ranging from 0.04 to 0.15 m for hip or shoulder pushes [11], [12] are comparable with our perturbation amplitudes. The perturbation torques at the ankle joint ranging from 1 to 16 Nm [13], [14] are also comparable with our induced perturbation torque, when assuming the mass of the participant was not taken into account. This shows that in general the used perturbation amplitudes in previous studies seem acceptable.

B. Quantifying Nonlinear Distortions

Since it is not possible to directly measure the bias due to nonlinear distortions ($G_B(f)$) on the estimation of the NMC, we calculated the stochastic nonlinear contributions ($G_S(f)$), which are of the same order as $G_B(f)$ [22].

Our results showed that the relative stochastic nonlinear contributions in the body sway due to nonlinear behavior of the NMC are only 2.3% for the even low frequencies and even lower (0.1%) for the odd mid frequencies, when detectable. Note that when stochastic nonlinear contributions are undetectable, the nonlinearities are small compared to the noise, which does not necessarily mean that they are not present. For the ankle torque, the relative stochastic nonlinear contributions due to nonlinear behavior of the NMC are only around 2% for the odd and even low frequencies and around 1% for the odd and even mid frequencies, when detectable. The odd and even high frequencies, however, showed more relative stochastic nonlinear contributions of 1.1-3.4%. The relative stochastic nonlinear contributions in the ankle torque do not change by increasing the perturbation amplitude.

Based on the results of van der Kooij [1], we expected the relative stochastic nonlinear contributions to be higher at high perturbation amplitudes. Especially at the higher perturbation amplitudes at which participants could not withstand the perturbation by keeping their feet in place. However, the relative nonlinear contributions did not increase at higher perturbation amplitudes. Since the relative nonlinear contributions did not increase at higher perturbation amplitudes, we assume that the nonlinear behavior due to a change in strategy, i.e. stepping, did not play a role yet. The fact that all participants could withstand the A20 condition supports this idea. The nonlinearities could be introduced by the nonlinear properties of a single inverted pendulum. However, the relative stochastic nonlinear contributions corresponding to the measured ptp body sway are too small to explain our results. Other explanations for the nonlinearities could be the nonlinear dynamics of the muscle such as short range stiffness or tendon stiffness, or the existence of thresholds in the NMC [1], [29], [30].

C. Variance Accounted For

To study the effect of both the relative variability, i.e. precision, and nonlinear distortions (G_B) on $G_{BLA}(f)$, the VAF was calculated to show how well the estimated linear model G_{BLA} describes the measured data. The VAF increased from $61\pm15\%$ to $93\pm2\%$ by increasing the perturbation amplitude. It remains unclear whether the VAF increases due to better NSR or due to the reduction of nonlinear distortions (G_B). Nevertheless, the VAF shows that up to 93% of the data could be explained by a linear model when using a perturbation amplitude of A17 or A20.

D. Limitations

The treadmill introduces nonlinear distortions in the perturbation torque (Fig 2, upper row). Nonlinear distortions in the perturbation torque due to nonlinear behavior of the treadmill might be interfering with the linear system identification techniques. However, with the method of

Schoukens and Pintelon [20], the body sway and ankle torque are corrected for the impurities. As the correction is not perfect, it would be best to limit the amount of nonlinear distortions in the perturbation torque.

The experiments in this study were performed with mainly healthy young participants. When studying populations with balance deficits, the variability between participants would probably be higher. In this case, we suggest a larger study population rather than higher perturbation amplitudes or higher number of repetitions. The within-subject variability for these populations is harder to predict and should first be investigated which can be done using the method presented in this paper.

V. Conclusions

In this study, we provide guidance to choose the appropriate amplitude and number of repetitions of the perturbation signal used in system identification approaches. The minimal perturbation amplitude should be 0.05 m peak-to-peak, since lower perturbation amplitudes require too many repetitions. However, higher perturbation amplitudes are preferred because the precision of the estimation is better, i.e. the relative variability is lower, resulting in a better explanation of the data by a linear model. There is however no need to further increase the perturbation amplitude than 0.14 m peak-to-peak. Using more repetitions always results in better precision, but the minimal required number of repetitions depends on the chosen perturbation amplitude and the desired precision. Nonlinear contributions are not higher than 3.5% in the range of 0.02-0.20 m peak-to-peak and nonlinear contributions to the ankle torque do not change with perturbation amplitude. To conclude, when investigating changes in underlying mechanisms of balance control due to ageing or pathologies, such as Parkinson's disease and stroke, the NMC could be estimated with the use of linear system identification techniques despite the presence of nonlinearities.

References

[1] H. van der Kooij and E. de Vlugt, "Postural responses evoked by platform pertubations are dominated by continuous feedback," *J. Neurophysiol.*, vol. 98, no. 2, pp. 730–743, Aug. 2007.

[2] J. H. Pasma, T. A. Boonstra, S. F. Campfens, A. C. Schouten, and H. van der Kooij, "Sensory reweighting of proprioceptive information of the left and right leg during human balance control," *J. Neurophysiol.*, vol. 108, no. 4, pp. 1138–1148, Aug. 2012.

[3] D. Engelhart, A. C. Schouten, R. G. K. M. Aarts, and H. V. D. Kooij, "Assessment of multi-joint coordination and adaptation in standing balance: A novel device and system identification technique," *IEEE Trans. Neural Syst. Rehabil. Eng.*, vol. 23, no. 6, pp. 973–982, Nov. 2015.

[4] D. Engelhart *et al.*, "Adaptation of multijoint coordination during standing balance in healthy young and healthy old individuals," *J. Neurophysiol.*, vol. 115, no. 3, pp. 1422–1435, Mar. 2016.

[5] E. H. F. van Asseldonk *et al.*, "Disentangling the contribution of the paretic and non-paretic ankle to balance control in stroke patients," *Exp. Neurol.*, vol. 201, no. 2, pp. 441–451, Oct. 2006.

[6] T. A. Boonstra, A. C. Schouten, and H. van der kooij, "Identification of the contribution of the ankle and hip joints to multi-segmental balance control," *J. Neuroeng. Rehabil.*, vol. 10, no. 1, P. 23, Feb. 2013.

[7] T. A. Boonstra, J. P. P. van Vugt, H. van der Kooij, and B. R. Bloem, "Balance asymmetry in Parkinson's disease and its contribution to freezing of gait," *PLoS ONE*, vol. 9, no. 7, Jul. 2014, Art. no. e102493.

[8] K. Van Ooteghem, J. S. Frank, F. Allard, J. J. Buchanan, A. R. Oates, and F. B. Horak, "Compensatory postural adaptations during continuous, variable amplitude perturbations reveal generalized rather than sequence-specific learning," *Exp. Brain Res.*, vol. 187, no. 4, pp. 603–611, Jun. 2008.

[9] J. Ko, J. H. Challis, and K. M. Newell, "Postural coordination patterns as a function of rhythmical dynamics of the surface of support," *Exp. Brain Res.*, vol. 226, no. 2, pp. 183–191, Apr. 2013.

[10] J. Ko, J. H. Challis, and K. M. Newell, "Transition of COM–COP relative phase in a dynamic balance task," *Hum. Movement Sci.*, vol. 38, pp. 1–14, Dec. 2014.

[11] S. Hwang, P. Agada, T. Kiemel, and J. J. Jeka, "Identification of the unstable human postural control system," *Frontiers Syst. Neurosci.*, vol. 10, p. 22, Mar. 2016.

[12] T. Kiemel, Y. Zhang, and J. J. Jeka, "Identification of neural feedback for upright stance in humans: Stabilization rather than sway minimization," *J. Neurosci.*, vol. 31, no. 42, pp. 15144–15153, Oct. 2011.

[13] C. Maurer, T. Mergner, and R. J. Peterka, "Multisensory control of human upright stance," *Exp. Brain Res.*, vol. 171, no. 2, pp. 231–250, Nov. 2005.

[14] T. Mergner, C. Maurer, and R. J. Peterka, "A multisensory posture control model of human upright stance," *Prog. Brain Res.*, vol. 142, pp. 189–201, Jan. 2003.

[15] A. Alexandrov, A. Frolov, F. Horak, P. Carlson-Kuhta, and S. Park, "Feedback equilibrium control during human standing," *Biol. Cybern.*, vol. 93, no. 5, pp. 309–322, Nov. 2005.

[16] R. Johansson, M. Magnusson, and M. Akesson, "Identification of human postural dynamics," *IEEE Trans. Biomed. Eng.*, vol. 35, no. 10, pp. 858–869, Oct. 1988.

[17] T. Kiemel, K. S. Oie, and J. J. Jeka, "Slow dynamics of postural sway are in the feedback loop," *J. Neurophysiol.*, vol. 95, no. 3, pp. 1410–1418, Mar. 2006.

[18] S. Park, F. B. Horak, and A. D. Kuo, "Postural feedback responses scale with biomechanical constraints in human standing," *Exp. Brain Res.*, vol. 154, no. 4, pp. 417–427, Feb. 2004.

[19] R. J. Peterka, "Postural control model interpretation of stabilogram diffusion analysis," *Biol. Cybern.*, vol. 82, no. 4, pp. 335–343, Mar. 2000.

[20] J. Schoukens, R. Pintelon, Y. Rolain, and T. Dobrowiecki, "Frequency response function measurements in the presence of nonlinear distortions," *Automatica*, vol. 37, no. 6, pp. 939–946, Jun. 2001.

[21] R. Pintelon, J. Schoukens, *System Identification: A Frequency Domain Approach*, 2nd ed. Hoboken, NJ, USA: Wiley, 2012.

[22] J. Schoukens, R. Pintelon, Y. Rolain, *Mastering System Identification in 100 Exercises*, 2nd ed. Hoboken, NJ, USA: Wiley, 2012.

[23] K. Vanhoenacker, T. Dobrowiecki, and J. Schoukens, "Design of multisine excitations to characterize the nonlinear distortions during FRF-measurements," *IEEE Trans. Instrum. Meas.*, vol. 50, no. 5, pp. 1097–1102, Oct. 2001.

[24] M. P. Vlaar, T. Solis-Escalante, A. N. Vardy, F. C. T. van der Helm, and A. C. Schouten, "Quantifying nonlinear contributions to cortical responses evoked by continuous wrist manipulation," *IEEE Trans. Neural Syst. Rehabil. Eng.*, vol. 25, no. 5, pp. 481–491, May 2017.

[25] D. A. Winter, *Biomechanics and Motor Control of Human Movement*, 3rd ed. Hoboken, NJ, USA: Wiley, 2008.

[26] B. Koopman, H. J. Grootenboer, and H. J. de Jongh, "An inverse dynamics model for the analysis, reconstruction and prediction of bipedal walking," *J. Biomech.*, vol. 28, no. 11, pp. 1369–1376, Nov. 1995.

[27] D. Engelhart, T. A. Boonstra, R. G. K. M. Aarts, A. C. Schouten, and H. van der Kooij, "Comparison of closed-loop system identification techniques to quantify multi-joint human balance control," *Annu. Rev. Control*, vol. 41, pp. 58–70, Jan. 2016.

[28] B. Efron, R. J. Tibshirani, *An Introduction to the Bootstrap*, 1st ed., London, U.K.: Chapman, 1994.

[29] J. J. Collins and C. J. De Luca, "Open-loop and closed-loop control of posture: A random-walk analysis of center-of-pressure trajectories," *Experim. Brain Res.*, vol. 95, no. 2, pp. 308–318, Aug. 1993.

[30] C. W. Eurich and J. G. Milton, "Noise-induced transitions in human postural sway," *Phys. Rev. E, Stat. Phys. Plasmas Fluids Relat. Interdisc. Top.*, vol. 54, no. 6, pp. 6681–6684, Dec. 1996.